Supporting Information for "Anomalous Meltwater from Ice Sheets and Ice Shelves is a Historical Forcing"

Gavin. A. Schmidt[1], Anastasia Romanou[1], Lettie A. Roach[2,1], Ken Mankoff[3,1], Qian Li[4], Craig D. Rye[2,1], Maxwell Kelley[1], John Marshall[4], Julius J. M. Busecke[5]

[1]NASA Goddard Institute for Space Studies, New York, NY

[2]Center for Climate Systems Research, Columbia University, New York, NY

[3]Autonomic Integra LLC, New York, NY

[4]MIT, Cambridge MA

[5]Lamont-Doherty Earth Observatory, Columbia University, Palisades, NY

Contents of this file

Corresponding author: G. A. Schmidt, NASA GISS, 2880 Broadway, New York, NY 10025, USA (gavin.a.schmidt@nasa.gov)

Introduction

The Supporting Information gives further details of the construction of the input data for the freshwater anomalies and details of the model simulations referenced in the main text.

Input data construction

For Greenland, observed mass loss is provided by Mankoff et al. (2021) as the total mass balance of grounded ice. Mass balance comes from ice discharge outputs, basal mass balance outputs and estimates of the SMB, which in turn come from the average of three regional climate models. The ice discharge outputs come from estimates of ice thickness, velocity, and density across near-terminus flux gates (Mankoff et al., 2020), and the basal mass balance (Karlsson et al., 2021) comes from modeled mass loss at the bed from geothermal heating, frictional heating, and viscous dissipation of heat from surface runoff (i.e. the volume of subglacial conduits, (Mankoff & Tulaczyk, 2017)). Years when there is mass gain (for instance, 1996) are set to 0 and that amount added to following years so that no years have a negative contribution of anomalous freshwater.

For Antarctica, mass loss is provided by Slater et al. (2021), combining mass loss from grounded ice (via GRACE/GRACE-FO), and from direct annual observations of ice shelf thinning and calving. Mass balance of ice shelf calving is available annually from 1994 through 2001, and then from bulk changes from 2001 through 2016, applied annually between those dates. We extrapolate back to 1990 and forward through 2019 using the average of the first and last three years of the data, respectively.

The spatial masks as well as the annual and cumulative fluxes are shown in Figure S1. The uncertainty ranges are plausible estimates based on the published annual data for Greenland (Mankoff et al., 2021), and for Antarctica, the uncertainty of 78 Gt yr^{-1} is estimated from twice the largest uncertainty of the ice shelf calving, thinning, or land ice terms (Slater et al., 2021).

References

Hausfather, Z., Marvel, K., Schmidt, G. A., Nielsen-Gammon, J. W., & Zelinka, M. (2022a). Climate simulations: recognize the 'hot model' problem. *Nature*, *605*(7908), 26–29. doi: 10.1038/d41586-022-01192-2

Hausfather, Z., Marvel, K., Schmidt, G. A., Nielsen-Gammon, J. W., & Zelinka, M. (2022b). *Supporting information for Hausfather et al 2022, Climate simulations: recognize the 'hot model' problem, comment in Nature.* Zenodo. (v1.0 ; Accessed 2023-09-12 [Dataset]) doi: 10.5281/zenodo.6476375

Karlsson, N. B., Solgaard, A. M., Mankoff, K. D., Gillet-Chaulet, F., MacGregor, J. A., Box, J. E., . . . Fausto, R. S. (2021). A first constraint on basal melt-water production of the Greenland ice sheet. *Nature Communications*, *12*(3461). doi: 10.1038/s41467-021-23739-z

Lee, J.-Y., Marotzke, J., Bala, G., Cao, L., Corti, S., Dunne, J. P., . . . Zhou, T. (2021). Future global climate: Scenario-based projections and near-term information. In V. Masson-Delmotte et al. (Eds.), *Climate change 2021: The physical science basis. contribution of working group i to the sixth assessment report of the intergovernmental panel on climate change* (pp. 553–672). Cambridge, United Kingdom and New York, NY, USA: Cambridge University Press. doi: 10.1017/9781009157896.006

Mankoff, K. D., Fettweis, X., Langen, P. L., Stendel, M., Kjeldsen, K. K., Karlsson, N. B., . . . Fausto, R. S. (2021). Greenland ice sheet mass balance from 1840 through next week. *Earth System Science Data*, *13*(10), 5001–5025. doi: 10.5194/essd-13-5001-2021

Mankoff, K. D., Solgaard, A., Colgan, W., Ahlstrøm, A. P., Khan, S. A., & Fausto, R. S. (2020, 6). Greenland ice sheet solid ice discharge from 1986 through March 2020. *Earth System Science Data*, *12*(2), 1367-1383. doi: 10.5194/essd-12-1367-2020

Mankoff, K. D., & Tulaczyk, S. M. (2017). The past, present, and future viscous heat dissipation available for Greenland subglacial conduit formation. *The Cryosphere*, *11*, 303–317. doi: 10.5194/tc-11-303-2017

Miller, R. L., Schmidt, G. A., Nazarenko, L. S., Bauer, S. E., Kelley, M., Ruedy, R., ... Yao, M.-S. (2021). CMIP6 historical simulations (1850–2014) with GISS-E2.1. *Journal of Advances in Modeling Earth Systems*, *13*(1). doi: 10.1029/2019ms002034

Slater, T., Lawrence, I. R., Otosaka, I. N., Shepherd, A., Gourmelen, N., Jakob, L., ... Nienow, P. (2021). Review article: Earth's ice imbalance. *The Cryosphere*, *15*(1), 233–246. doi: 10.5194/tc-15-233-2021

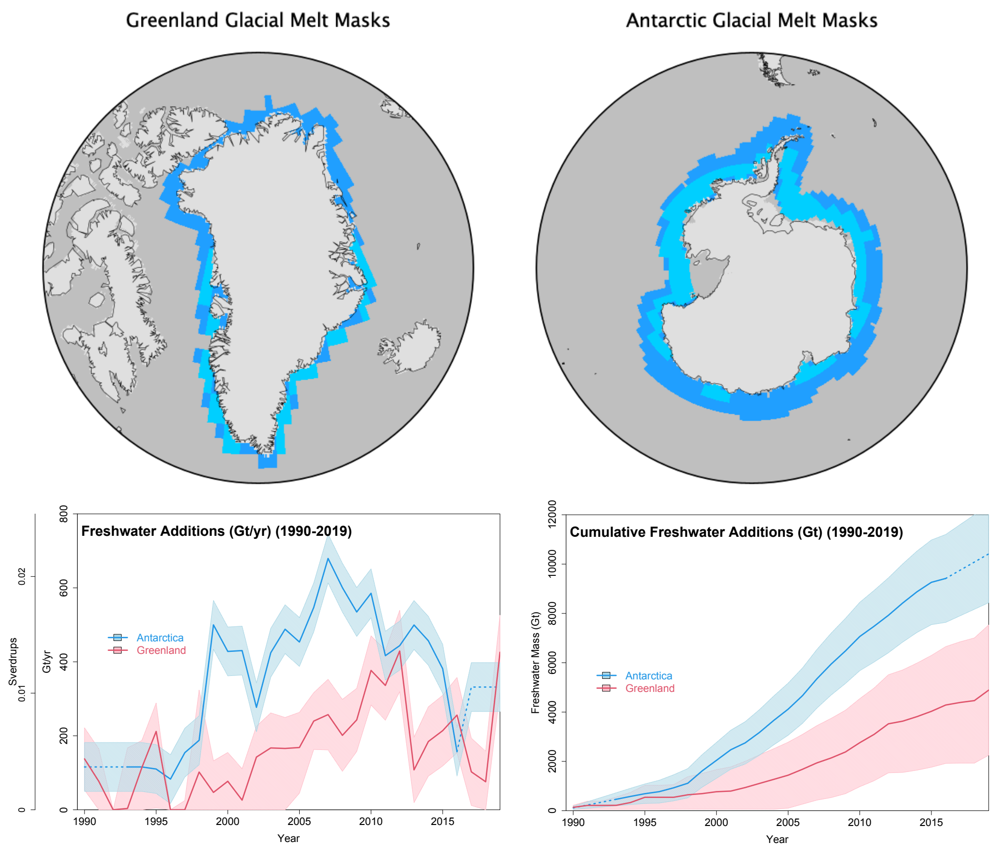

Figure S1. Top row: Glacial melt spatial masks around Greenland and Antarctica used in GISS-E2.1-G for adding climatological (light blue) and anomalous freshwater (dark blue plus light blue) from the ice sheets into the ocean. Bottom row: Anomalous total freshwater flux amounts used in these experiments (annual fluxes (Gt yr^{-1} or Sv) and cumulative fluxes (Gt) aggregated by hemisphere). Uncertainty bands are the spread in maximum and minimum plausible changes for each ice sheet. Antarctic values before 1994 and after 2015 are estimated using the mean of the post or prior three-year period (dashed lines).

Model	ripf number	DOI
ACCESS-CM2	r1i1p1f1	https://doi.org/10.22033/ESGF/CMIP6.4271
BCC-CSM2-MR	r1i1p1f1	https://doi.org/10.22033/ESGF/CMIP6.2948
CAMS-CSM1-0	r1i1p1f1	https://doi.org/10.22033/ESGF/CMIP6.9754
CESM2	r10i1p1f1	https://doi.org/10.22033/ESGF/CMIP6.7627
CESM2-WACCM	r1i1p1f1	https://doi.org/10.22033/ESGF/CMIP6.10071
CMCC-CM2-SR5	r1i1p1f1	https://doi.org/10.22033/ESGF/CMIP6.3825
CMCC-ESM2	r1i1p1f1	https://doi.org/10.22033/ESGF/CMIP6.4068
CNRM-ESM2-1	r10i1p1f2	https://doi.org/10.22033/ESGF/CMIP6.4068
FGOALS-f3-L	r1i1p1f1	https://doi.org/10.22033/ESGF/CMIP6.3355
FGOALS-g3	r1i1p1f1	https://doi.org/10.22033/ESGF/CMIP6.3356
GFDL-CM4	r1i1p1f1	https://doi.org/10.22033/ESGF/CMIP6.8594
GFDL-ESM4	r1i1p1f1	https://doi.org/10.22033/ESGF/CMIP6.8597
GISS-E2-1-G	r10i1p1f2	https://doi.org/10.22033/ESGF/CMIP6.7127
IITM-ESM	r1i1p1f1	https://doi.org/10.22033/ESGF/CMIP6.3708
INM-CM5-0	r1i1p1f1	https://doi.org/10.22033/ESGF/CMIP6.5070
MIROC-ES2L	r10i1p1f2	https://doi.org/10.22033/ESGF/CMIP6.5602
MIROC6	r10i1p1f1	https://doi.org/10.22033/ESGF/CMIP6.5603
MPI-ESM1-2-HR	r1i1p1f1	https://doi.org/10.22033/ESGF/CMIP6.6594
MPI-ESM1-2-LR	r10i1p1f1	https://doi.org/10.22033/ESGF/CMIP6.6595
MRI-ESM2-0	r1i1p1f1	https://doi.org/10.22033/ESGF/CMIP6.6842
NorESM2-LM	r1i1p1f1	https://doi.org/10.22033/ESGF/CMIP6.8036

Table S1. The 21 model simulations from CMIP6 that were used in the construction of Fig. 1b (using the historical and ssp245 experiments), screened for TCR values in the likely range 1.4–2.2ºC (Hausfather et al., 2022a), as defined by Lee et al. (2021), and with TCR values from Hausfather et al. (2022b). Single ensemble members from each model were selected based on availability and appropriate meta-data.

Simulation ripf numbers	Location
r20[1-10]i1p1f[24]	https://portal.nccs.nasa.gov/datashare/giss_cmip6/ https://doi.org/10.22033/ESGF/CMIP6.7127

Table S2. The extended historical GISS-E2.1-G model simulations used in this paper (using standard regexp notation). The 'f2' (forcing) variant denotes the standard forcing as used in Miller et al. (2021), and 'f4' is the forcing variant including the anomalous freshwater.